

MEASUREMENT OF LIGHT-CONE WAVE FUNCTIONS BY DIFFRACTIVE DISSOCIATION

DANIEL ASHERY

*School of Physics and Astronomy, Sackler Faculty of Exact Science,
Tel Aviv University, Tel Aviv 69978, Israel*

The measurement of the pion light-cone wave function is revisited and results for the Gegenbauer coefficients are presented. Measurements of the photon electromagnetic and hadronic wave functions are described and results are presented.

1 The Pion Light Cone Wave Function

A differential measurement of the pion LCWF was performed by Fermilab E791 collaboration¹ by studying the diffractive dissociation of 500 GeV/c pions, interacting with C and Pt targets, to two jets. If in this process the quark momentum is transferred to the jet, measurement of the jet momentum gives the quark (and antiquark) momentum. Thus: $u_{\text{measured}} = \frac{p_{\text{jet1}}}{p_{\text{jet1}} + p_{\text{jet2}}}$.

It has been shown² that the cross section for this process is proportional to ϕ^2 . The resulting u distributions are shown in Fig. 1 for two windows of k_t : $1.25 \text{ GeV/c} \leq k_t \leq 1.5 \text{ GeV/c}$ and $1.5 \text{ GeV/c} \leq k_t \leq 2.5 \text{ GeV/c}$. The results are compared with linear combinations of simulations of squares of the asymptotic³ and CZ⁴ distribution amplitudes.

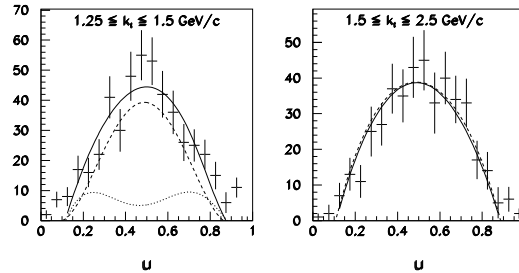


Figure 1: The u distribution of diffractive di-jets from the platinum target. The solid line is a fit to a combination of the asymptotic and CZ wave functions. The dashed line shows the contribution from the asymptotic function and the dotted line that of the CZ function.

The results for the higher k_t window show that the asymptotic wave function describes the data very well. Hence, for $k_t > 1.5 \text{ GeV/c}$, which translates to $Q^2 \sim 10 \text{ (GeV/c)}^2$, the pQCD approach that led to construction of the asymptotic wave function is reasonable. The distribution in the lower window is consistent with a significant contribution from the CZ wave function or may indicate contributions due to other non-perturbative effects. A way to understand this better is to use the experimental results to determine the coefficients of the Gegenbauer polynomials in the expansion of $\phi_\pi(u, Q^2)$ ³. One cannot fit directly the results shown in Fig. 1 as these are distorted by the hadronization process and experimental acceptance. It is also not practical to carry out simulations of the distortions for a large variety of distribution amplitudes. We adopt here a simpler approach, albeit somewhat less precise than that used by E791. We use

results of the Monte Carlo simulations to correct the distortions and experimental acceptance⁵. The results, Fig. 2, are fitted to the expression:

$$\frac{d\sigma}{du} \propto \phi_\pi^2(u, Q^2) = N \cdot u^2(1-u)^2 \times \left(1.0 + a_2 C_2^{3/2}(2u-1) + a_4 C_4^{3/2}(2u-1)\right)^2 \quad (1)$$

where N is a normalization constant and C_n are the Gegenbauer polynomials. The results of the fits are that for the high k_t region $a_2 = a_4 = 0$, confirming the conclusion of the E791 authors that for this region ϕ_{Asy}^2 describes the data well. For the low k_t region the coefficients are: $a_2 = 0.30 \pm 0.05$, $a_4 = (0.5 \pm 0.1) \cdot 10^{-2}$. The fact that $a_4 \neq 0$ indicates a distribution amplitude that is different from ϕ_{CZ} which contains only an a_2 term. The k_t dependence of diffractive

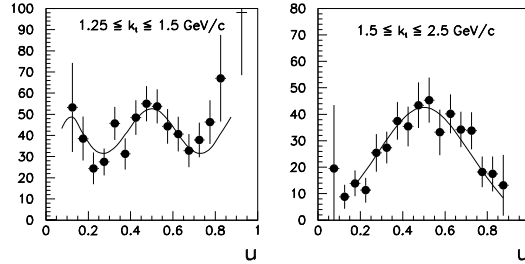


Figure 2: The Acceptance-corrected u distributions of diffractive di-jets obtained by applying correction to the E791 results¹. The solid line is a fit to a combination of Gegenbauer polynomials, Eq. 1.

di-jets is another observable that can show the region where perturbative calculations describe the data. As shown in² it is expected to be: $\frac{d\sigma}{dk_t} \sim k_t^{-6}$. The results, shown in Fig. 3, are consistent with this dependence only in the region above $k_t \sim 1.8$ GeV/c, in agreement with the conclusions from the u -distributions. For lower k_t values, non-perturbative effects are expected to be significant. Naturally, the transition between the two regions is not sharp. The region of $1.0 \leq k_t \leq 1.8$ GeV/c may be a transition region where we can still apply pQCD techniques but must use LCWFs that better describe the non-perturbative structure of the pion. In Fig 3(a)

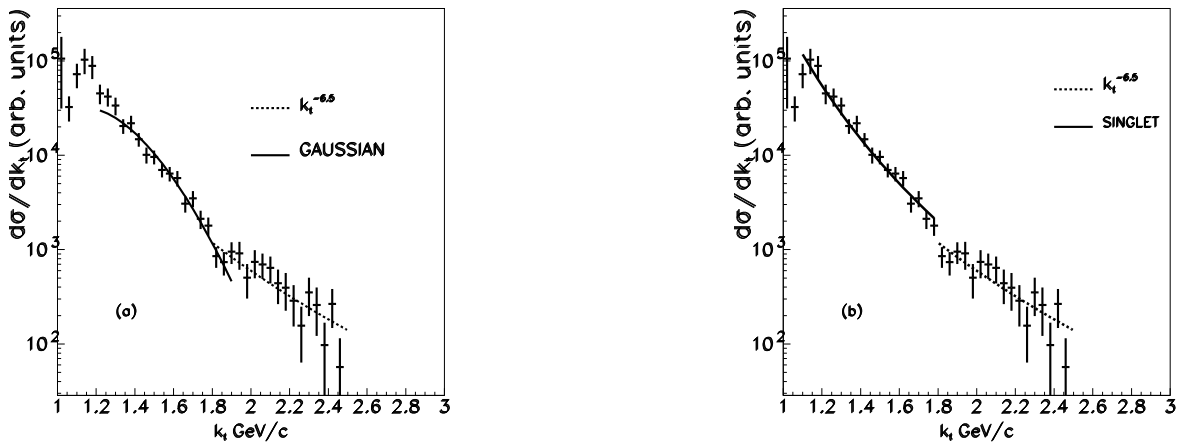


Figure 3: Comparison of the experimental k_t distribution¹ with fits derived from: (a) Gaussian LCWF⁶ for low k_t and a power law dependence: $\frac{d\sigma}{dk_t} \propto k_t^n$, as expected from perturbative calculations, for high k_t ; (b) Two-term Singlet model wave function⁷ for low k_t and a power law for high k_t .

it is compared with a Gaussian wave function⁶ and in Fig 3(b) to the a Singlet model wave function⁷. The observed sensitivity shows that the k_t distribution is useful in studying wave functions in this transition region.

2 The Photon Light Cone Wave Function

2.1 Measurement of the electromagnetic component of real photon LCWF

This is the well known Bethe-Heitler process. Using the LCWF formalism it has been shown⁵ that the cross section for real photons and using $m_l = 0 \rightarrow a = 0$ is:

$$\frac{d\sigma}{dt du dk_t^2} \propto \frac{2[u^2 + (1-u)^2]}{k_t^4} \sim \frac{\Phi^2}{k_t^2}. \quad (2)$$

This proportionality can be utilized in the same way as was done for the pion. Measurement of the photon light-cone wave function was carried out at the DESY accelerator in the collision of 28 GeV/c electrons (or positrons) with 920 GeV/c protons producing real or virtual photons. The measurements were done with the ZEUS detector⁸ using the exclusive $ep \rightarrow e\mu^+\mu^-p$ photoproduction process. The integrated luminosity for the results was $55.4 \pm 1.3 \text{ pb}^{-1}$. The kinematic region was defined by the following selection criteria: the invariant mass of the dimuon system $4 < M_{\mu\mu} < 15 \text{ GeV}$ (above the resonances), the γp centre of mass energy $30 < W < 170 \text{ GeV}$ (region of stable and high acceptance), the square of the four momentum exchanged at the proton vertex $|t| < 0.5 \text{ GeV}^2$ (select diffractive events), $0.1 < u < 0.9$ (avoid the end-points region with low acceptance) and $k_T > 1.2 \text{ GeV}$ (select a hard process). The measured differential cross section $d\sigma/du$ is presented in Fig. 4 and is in good agreement with the LCWF squared (BFGMS)⁹. This measurement serves as “Standard Candle” and normalization for the Hadronic LCWF. It also provides the first proof that diffractive dissociation of particles can be reliably used to measure their LCWF. Furthermore it gives support for the method used in previous measurements of the pion LCWF¹ and possible future applications to other hadrons^{5,10}.

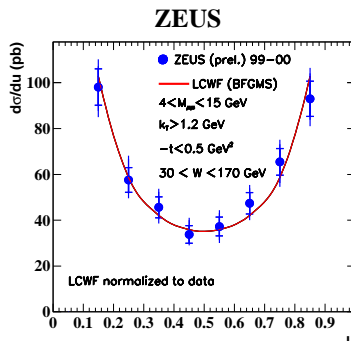


Figure 4: Differential cross section $d\sigma/du$ measured for the selected kinematic region (see text). The inner error bars show the statistical uncertainty; the outer error bars show the statistical and systematics added in quadrature. The data points are compared to the prediction of LCWF theory. The theory is normalized to data.

2.2 Measurement of the hadronic component of the photon LCWF by Exclusive Dipion Electroproduction

The processes of photo- or electro-production of two pions may be considered as a special case of the photon dissociation to dijets when each jet consists of one pion (Fig. 5). This is a very exclusive process where the pion form factor and quantum numbers may affect the ratio of longitudinal/transverse cross sections and the u -distribution. The cross section for this process

is expected to be proportional to the time-like form factor:

$$\frac{\sigma(\gamma^* + p \rightarrow 2\pi + p)}{\sigma(\gamma^* + p \rightarrow X + p)} \propto |F_\pi|^2 \quad (3)$$

where the denominator can be taken from parametrization of measurements and the results may have to be normalized to those obtained from e^+e^- measurements¹⁵. It may be possible to use these measurements to extend measurements of the pion time-like form factor into the $4 < Q^2 < 15$ region where there is great sensitivity to the pion light-cone wave function¹¹. The

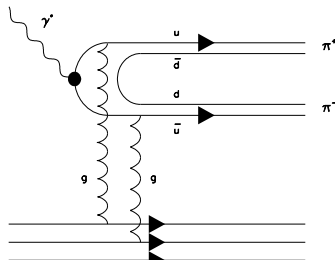


Figure 5: The photon dissociation to $q\bar{q}$ followed by hadronization to two pions

exclusive dipion reaction is considered as one of the ways to hunt for the elusive Odderon^{12,13} described as a d-coupled three-gluon color singlet $C = -1$ object¹⁴. Since the charge parity of dipions is: $C(\pi^+\pi^-) = (-)^\ell$ where ℓ is their relative angular momentum, both Pomeron and Odderon can contribute to their production and interference will show up. The signature would be charge asymmetry: $A = \frac{u(+)-u(-)}{u(+)+u(-)}$. It was calculated for dipion electroproduction¹² and photoproduction¹³. Measurement of exclusive diffractive electroproduction of $\pi^+\pi^-$ pairs was carried out by the ZEUS collaboration with integrated luminosity of $66.3 \pm 1.7 \text{ pb}^{-1}$. The kinematic conditions for this measurement were: $2 < Q^2 < 20 \text{ GeV}^2$, $1.2 < M_{\pi\pi} < 5 \text{ GeV}$, $40 < W < 120 \text{ GeV}$, $|t| < 0.5 \text{ GeV}^2$, $0.1 < u < 0.9$. The mass distribution, when divided by the mass dependence of the $\gamma^*p \rightarrow q\bar{q}$ cross section can be used to extend the measurements of the time-like form factor from the highest available value at 2 GeV¹⁵ up to about 4 GeV. The t distribution is fitted with the standard exponential form $d\sigma/dt \propto e^{bt}$. The resulting slope $b = -4.81 \pm 0.42(\text{stat})_{-0.44}^{+0.05}(\text{sys}) \text{ GeV}^{-2}$ is in good agreement with the values observed for vector-meson production¹⁶. This slope is considered as a measure of the combined size of the $q\bar{q}$ system and the proton: $b = \frac{1}{3} < R^2 > + \frac{1}{8}r^2$ where $r \sim \frac{6}{\sqrt{Q^2+m_V^2}}$ is the size of the $q\bar{q}$ system before it hadronizes to a vector meson or, in this case, to two pions in the continuum and R is the proton radius¹⁷. The results show that the $q\bar{q}$ size in hadronization to continuum states is similar to that obtained for vector mesons.

The u distribution is presented in Fig. 6 for two Q^2 intervals. Its shape is compared to the LCWF predictions for transverse and longitudinal photons⁵. Such a comparison is legitimate if the pion quantum numbers do not affect their angular (u) distributions for a given photon polarization. The normalization for the longitudinal LCWF prediction was determined from fit to the data. For the transverse LCWF prediction it was fixed to be the same value as that for the longitudinal prediction at $u = 0.5$. We note that the measured distribution in the low Q^2 region (Fig. 6 left) is more irregular than the one for the higher Q^2 range. This irregularity can be traced to the fact that the low Q^2 range is close to the average value of the dipion mass squared. In fact, for this range $\langle \beta \rangle = 0.52$ which is where $\sigma_L/\sigma_T \sim 0$ in leading order⁵. Higher order effects are expected to play a role here and the pure longitudinal fluctuations may be shadowed. By contrast, for the high Q^2 range $\langle \beta \rangle = 0.75$ which is a “safe” region.

The results are consistent with the LCWF predictions for longitudinally polarized photons. The agreement between the measured u distributions and the predictions lends support to the assumption that non-resonant di-pion production is sensitive to the $q\bar{q}$ component of the light-cone wave function of the virtual photon. This shows that for the phase space parameters of this study the LCWF predicted by perturbative QCD is correct. This process of exclusive diffractive electroproduction of pion pairs can be correctly described as resulting from a longitudinal photon fluctuating to a $q\bar{q}$ pair which in turn hadronizes to a $\pi^+\pi^-$ pair, Fig. 5. The agreement of the u -distribution measured with pions in the continuum and in the resonance region above the ρ with calculations made at the parton level lend support to the picture that there is parton/hadron duality,¹⁸.

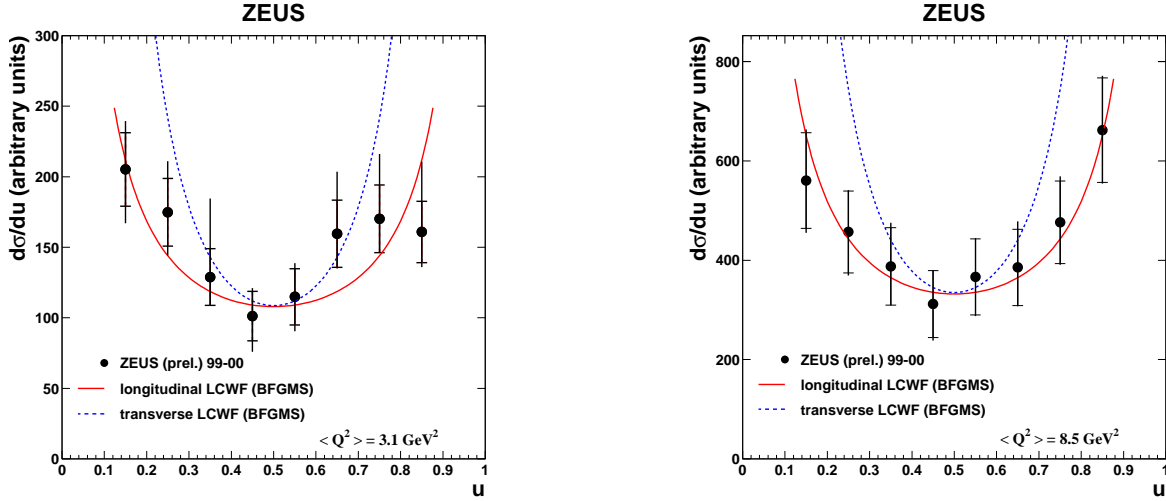


Figure 6: The differential cross section $d\sigma/du$ measured in two Q^2 intervals: $2 < Q^2 < 5 \text{ GeV}^2$ (left) and $5 < Q^2 < 20 \text{ GeV}^2$ (right). The inner error-bars show the statistical uncertainties; the outer error-bars show the statistical and systematic uncertainties added in quadrature. The data points are compared to the LCWF predictions.

1. E791 Collaboration, E.M. Aitala *et al.*, Phys. Rev. Lett. **86**, 4773 (2001)
2. L.L. Frankfurt, G.A. Miller, and M. Strikman, Phys. Lett. **B304**, 1 (1993).
3. S.J. Brodsky and G.P. Lepage, Phys. Rev. **D22**, 2157 (1980)
4. V.L. Chernyak and A.R. Zhitnitsky, Phys. Rep. **112**, 173 (1984).
5. D. Ashery, Prog. Part. Nucl. Phys. (in press)
6. R. Jakob and P. Kroll, Phys. Lett. **B315**, 463 (1993).
7. D. Ashery and H.C. Pauli, Eur. Phys. J. **c28**, 329 (2003)
8. ZEUS Coll., U.Holm *et al.*, The ZEUS Detector (unpublished) DESY 1993, www-zeus.desy.de/bluebook/bluebook.html
9. S. J. Brodsky, L. Frankfurt, J.F. Gunion, A.H. Mueller and M. Strikman, Phys. Rev. **D50**, 3134 (1994)
10. D. Ashery, Comments on Modern Physics **2A**, 235 (2002).
11. T. Gousset and B. Pire, Phys. Rev. **D51**, 15 (1995)
12. Ph. Hagler *et al.*, Phys. Lett. **B535**, 117 (2002)
13. I.F. Ginzburg, I.P. Ivanov and N.N. Nikolaev Eur. Phys. J. **C32** (Direct), s23 (2003)
14. L. Lukaszuk and B. Nicolescu, Lett. Nuovo Cim., **8**, 405 (1973); D. Joyson *et al.*, Nuovo Cim. **A30**, 345 (1975)
15. DM2 Collaboration D. Bisello *et al.* Phys. Lett. **B220**, 321 (1989)
16. A. Levy, proceedings of the Diffraction 2004 workshop, Cala Gonone, sardinia, Italy (2004).

17. N.N. Nikolaev, B.G. Zakharov, V.R. Zoller, Phys. Lett. **B366**, 337 (1996), J. Nemchik *et al.*, JETP **86**, 1054 (1998)
18. F.E. Close and N. Isgur, Phys. Lett. **B509**, 81 (2001)